Journal of Applied Polymer Science

WILEY

Applied Polymer SCIENCE

RESEARCH ARTICLE OPEN ACCESS

Predicting Mechanical Properties of FDM-Produced Parts Using Machine Learning Approaches

Mahmut Özkül[1] | Fatma Kuncan[1] | Osman Ulkir[2]

[1]Department of Computer Engineering, Siirt University, Siirt, Turkey | [2]Department of Electric and Energy, Mus Alparslan University, Mus, Turkey

Correspondence: Osman Ulkir (o.ulkir@alparslan.edu.tr)

Received: 7 January 2025 | **Revised:** 3 February 2025 | **Accepted:** 4 February 2025

Funding: The authors received no specific funding for this work.

Keywords: Mechanical Properties | Surfaces and Interfaces | Thermoplastics

ABSTRACT

Additive manufacturing (AM), especially fused deposition modeling (FDM), has been widely used in industrial production processes in recent years. The mechanical properties of parts produced by FDM can be predicted through the correct selection of printing parameters. In this study, 25 machine learning (ML) algorithms were used to predict the mechanical properties (hardness, tensile strength, flexural strength, and surface roughness) of acrylonitrile butadiene styrene (ABS) samples fabricated by FDM. Experiments were conducted using three different layer thicknesses (100, 150, 200 μm), infill densities (50%, 75%, 100%), and nozzle temperatures (220°C, 230°C, 240°C). The effects of printing parameters on mechanical properties were investigated through analysis of variance (ANOVA). This analysis results indicated that infill density had the most significant effect on hardness (55.56%), tensile strength (80.02%), and flexural strength (77.13%). In addition, the layer thickness was identified as the most influential parameter on the surface roughness, with an effect of 70.89%. The prediction performance of the ML algorithms was evaluated based on the mean absolute error (MAE), root mean squared error, mean squared error, and *R*-squared (R^2) values. The KSTAR algorithm best predicted both hardness and surface roughness, with MAE values of 0.006 and 0.009, respectively, and an R^2 value of up to 0.99. For the prediction of tensile and flexural strength, the MLP algorithm was determined to be the most successful method, achieving high accuracy ($R^2 > 0.99$) for both properties. In addition, comparison graphs between the predicted and actual results showed high overall accuracy, with a particularly strong agreement for hardness, tensile strength, and surface roughness. The study identified the algorithms with the best prediction performance and provided recommendations for predicting the 3D printing process based on these findings.

1 | Introduction

Additive manufacturing (AM) is a rapidly advancing production technology that has gained traction across various industrial fields in recent years [1, 2]. This technology enables the fabrication of parts by adding layers, allowing for the cost-effective production of complex geometries compared with traditional manufacturing methods. The flexibility and design freedom offered by AM have led to its widespread application, particularly in the fields of prototyping, automotive, aerospace, and medicine [3–6]. However, realizing the full potential of AM requires a precise determination of the production parameters and an understanding of how they affect the mechanical properties of the parts [7]. In this regard, optimizing production parameters based on their effects can lead to improved product quality and cost efficiency [8].

Fused deposition modeling (FDM), an AM technique, is especially favored for its compatibility with thermoplastic materials [9–11]. FDM has gained significant traction in the industrial

and academic sectors because of its relatively low cost, wide material range, and broad applicability—from prototype production to functional part fabrication [12, 13]. The materials commonly used in FDM are thermoplastic polymers, with high-performance engineering materials such as acrylonitrile butadiene styrene (ABS), polylactic acid (PLA), and polyethylene terephthalate glycol (PETG) being among the most widely utilized [14, 15]. FDM is a technology in which the production parameters play a critical role in the print quality and mechanical properties [16, 17]. Factors like layer thickness, infill density (ID), and nozzle temperature (NT) directly affect the print quality and mechanical characteristics of the final product [18, 19]. Mechanical properties such as hardness, tensile strength, flexural strength, and surface roughness can be optimized through proper adjustment of these parameters [20–22]. In contrast, incorrect parameter selection can lead to print errors, low strength values, and a decrease in overall product quality. Optimizing printing parameters in FDM technology is crucial for minimizing print time and cost while ensuring that the mechanical properties meet expectations [23]. Therefore, each printing parameter directly influences the performance of the final product, and optimizing these parameters enables FDM to be used more effectively across a wide range of applications.

In recent years, machine learning (ML) methods have become valuable tools for predicting and optimizing AM processes [24–26]. ML enables more accurate modeling of the manufacturing process by working with large datasets and can predict the effects of specific parameters (such as print speed [PS], layer height [LH], and NT) on the final properties of products. This approach makes it possible to enhance process efficiency by reducing production time, minimizing material waste, and lowering energy consumption. ML techniques can understand complex data relationships, learn the dynamics of processes, and forecast future outcomes without human intervention [27]. This ability is particularly valuable in AM processes, where parameters have a direct impact on mechanical properties and numerous factors interact simultaneously. Consequently, ML helps improve product quality, reduces production costs, and optimizes processes, thereby facilitating the adoption of economically and environmentally sustainable manufacturing methods.

Studies on the application of ML algorithms in AM demonstrate the effectiveness of these technologies in optimizing production processes [28–32]. Cerro et al. applied ML algorithms to predict the surface roughness of parts produced by FDM using polyvinyl butyral material [33]. Five input variables were determined, and 16 parts were 3D printed with three different surfaces; the surface roughness was then measured. A total of 40 models were trained and validated, with the best results obtained using bagging and a backpropagation multi-layer perceptron. Raster angle and LH were identified as the most influential parameters on surface quality. Hooda et al. employed a random forest ML model to predict the ideal placement angle in FDM based on product geometry [34]. Training data were created using different shapes and geometries, and significant features were selected using a correlation-based feature selection technique. The model's effectiveness was tested using K-fold cross-validation, achieving 94.57% accuracy. Winson et al. investigated the 3D printing of PLA composites reinforced with 4.6 mm chopped carbon fiber (CF) using FDM [35]. As the CF content increased, properties such as tensile and flexural strength, hardness, and thermal conductivity improved significantly compared with pure PLA. The performance exhibited a rise-fall-rise trend with CF addition, and Gaussian process modeling predicted the optimal CF content of 6.7 wt%, which was closely aligned with the experimental results. Charalampous et al. aimed to develop a new parameter selection method to improve the dimensional accuracy of FDM-produced parts [36]. Using ML algorithms, the method predicts the dimensional deviations between the CAD models and the fabricated parts. Experiments conducted under various printing conditions demonstrated the effectiveness of the regression models in suggesting print settings and correcting errors. This study presents the first ML-based regression models and correction strategies for assessing and improving FDM process quality. Ulkir used carbon black-filled ABS material for 3D printing using the FDM process [37]. Tensile tests were conducted to determine the mechanical strength, whereas resistance tests were carried out to assess electrical conductivity. Factors affecting strength included ID and LH; infill pattern (IP); for electrical resistance, significant factors were length, NT, and measurement temperature. The data were analyzed, and predictive models for tensile strength and electrical resistance were developed using Gaussian process regression and support vector machine algorithms. Results revealed a linear relationship between electrical resistance and length, as well as the impact of manufacturing settings on mechanical strength. However, while these studies provide valuable insights, many focus on limited ML algorithms or specific mechanical properties, such as surface roughness or dimensional accuracy, without comprehensively exploring other key properties like tensile or flexural strength. Moreover, the interaction effects of critical printing parameters, such as LH, ID, and NT, remain underexplored in the context of multi-property optimization. The potential research gap lies in the need for a broader analysis of ML algorithms across multiple mechanical properties and their ability to predict the combined effects of diverse printing parameters. While existing studies demonstrate the feasibility of ML in AM, the lack of a comprehensive evaluation of multiple algorithms for simultaneous prediction of properties such as hardness, tensile strength, flexural strength, and surface roughness represents a critical gap. This study seeks to address this gap by employing 25 different ML algorithms to predict these properties and by analyzing the impact of key printing parameters using analysis of variance (ANOVA). The rationale behind this work is to provide a more holistic understanding of the predictive capabilities of ML in AM, establish recommendations for algorithm selection, and optimize printing processes to improve the quality and reliability of FDM-produced ABS parts. This approach builds upon existing literature while filling the identified research gap through a systematic and comprehensive evaluation.

This study aimed to predict the mechanical properties, such as hardness, flexural strength, tensile strength, and surface roughness, of ABS samples produced using the FDM. Experiments were conducted by selecting the printing parameters of layer thickness, ID, and NT to achieve this goal. The effects of these parameters on the mechanical properties and roughness were statistically evaluated using ANOVA. Data obtained from the experiments were modeled using 25 different ML algorithms, and the prediction performances of these algorithms were assessed based on the mean absolute error (MAE), root mean squared

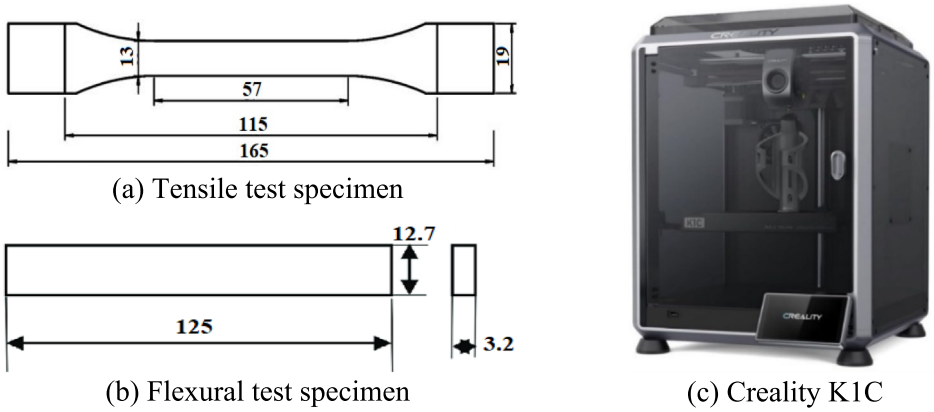

FIGURE 1 | The sample dimensions (mm) and FDM-based 3D printer. [Color figure can be viewed at wileyonlinelibrary.com]

TABLE 1 | The constant 3D printing parameters during AM.

Parameter	Unit	Value
Nozzle diameter	mm	0.4
Table temperature	°C	90
Number of contours	integer	7
Raster width	mm	0.40
Infill pattern	—	Grid
Printing speed	mm/s	90
Wall thickness	mm	3

error (RMSE), mean squared error (MSE), and *R*-squared (R^2) values. The algorithms with the best prediction performance were identified, and optimization recommendations for the 3D printing process were provided considering these results.

2 | Materials and Methods

2.1 | AM Process

In this study, the fabrication of tensile and flexural test specimens was performed using the FDM method. This method is a widely used AM technique that enables the physical production of 3D models by heating and extruding thermoplastic materials through a nozzle layer by layer [38]. The printer used in the production process was a Creality K1C model (Figure 1c). This 3D printer is known for its high printing speed and precision. With a maximum printing speed of 600 mm/s and a melt extrusion rate of 32 mm^3/s, this printer allows for the rapid and accurate production of complex geometries. The NT of the printer can reach up to 300°C, and the build platform can be heated up to 100°C, providing a compatible environment for a wide range of materials. In this study, the material used was ABS, selected for its high durability, hardness, and heat-resistance properties [39, 40].

The tensile test specimens were designed in accordance with the ASTM D638 standard (Figure 1a). This standard specifies the dimensions and geometric characteristics of specimens used in tensile tests. The specimens were modeled in 3D using SolidWorks software, and the models were exported in standard triangle language (STL) format. This format records the surface geometry by triangulating the model and aids in generating the layered structure necessary for 3D printing. The STL file was then transferred to the slicing software, and parameters such as LT, PS, and NT were defined. Following the slicing process, a G-code file was generated, which controls the printer's movement paths and material flow. Using this G-code file, the 3D printer melted the ABS material at the specified temperature and produced the tensile test specimens' layer by layer in accordance with the ASTM D638 standard. The flexural test specimens were designed in accordance with the ASTM D790 standard (Figure 1b). This study also examines other mechanical properties, including hardness and surface roughness, using tensile test specimens. Twenty-seven test specimens were produced for each mechanical property according to experimental design. All samples were printed on the XY plane and loaded in the Z direction. Based on the design of experiments approach, variable 3D printing parameters and levels were determined. In addition, other parameters were kept constant during the production process. The constant 3D printing parameters are detailed in Table 1.

2.2 | Measurement of Mechanical Properties

In the ML process, four mechanical properties were examined as output parameters: tensile strength, flexural strength, hardness, and surface roughness. Mechanical measurements were conducted on the ABS material produced using FDM. The tensile strength refers to the maximum amount of stress a material can withstand without breaking under tension. Tensile tests were performed on a 50-kN capacity AG-X Shimadzu device according to ASTM D638 standards at a pull speed of 1 mm/s. This device complies with ISO 7500/1, ASTM E4, and DIN51221 standards and provides results with ±0.1% accuracy. Flexural strength refers to the maximum stress a material can withstand when bending without breaking. Flexural tests were conducted on a 50-kN capacity AGS-X Shimadzu device, following ASTM D790 standards. The three-point bending method was applied using a fixed diameter mandrel and supports. ABS samples were bent at a speed of 1 mm/s using the mandrel. Hardness refers to a material's resistance to an applied force on its surface, typically related to its resistance to scratching or permanent deformation. Hardness measurements

were taken with a TRONIC PD-801 Analog Shoremeter, which is capable of measuring on the Shore D scale. According to the ASTM standards, measurements were taken from five points on both the top and bottom surfaces of the samples. The average of these values with a 1 kg/cm^2 (9.8 N) applied pressure on the surface was used to calculate the general hardness value. Surface roughness defines microscopic irregularities or small-scale protrusions and depressions on the surface. Surface roughness measurements were completed using the Mitutoyo Surftest SJ-210 device with a sampling length of 2.5 mm and measurement speed of 0.75 mm/s. Five measurements were performed for each sample. These tests provided reliable results by ensuring repeatability through multiple-point measurements, which helped analyze the mechanical and surface properties of the ABS material.

2.3 | Design of the Experiment

In AM processes, the printing parameters significantly affect the mechanical properties of the final product components. In this study, the three most important parameters affecting the mechanical properties were selected. These are LT, ID, and NT. LT refers to the height of each printed layer in the 3D printing and AM processes [41]. ID is a ratio that determines how solid or empty the interior of an object will be in 3D printing [42]. NT indicates the temperature at which the molten material is heated before being applied to the print surface in 3D printers [43]. These parameters were used as input variables in the ML implementation. Three levels were defined for each parameter. The other 3D printer parameters required for the manufacturing process were kept constant throughout the experimental stages. The input parameters and their level values for the ML algorithm are listed in Table 2.

Experimental combinations were created based on the identified input and output parameters. The present study includes three factors, each with three levels, resulting in 27 experimental runs. The data set prepared for the ML algorithm is presented in Table 3. Each output parameter in the proposed dataset represents an average of five repeated measurements for improved accuracy and reliability.

3 | ML Methodology

3.1 | Methods of Prediction

ML is the capability of a program to learn from new data and adapt without human intervention [44, 45]. An ML model analyzes the relationship between process factors and outputs. In this study, regression strategies were employed to perform computations aimed at predicting the output responses obtained through 3D printing, namely hardness, tensile strength, surface roughness, and flexural strength. ML methods are classified into five main groups: functional algorithms, lazy learning algorithms, meta-learning algorithms, rule-based algorithms, and tree-based algorithms. Table 4 lists the full names of the 25 ML algorithms considered in this study.

The dataset created for the ML algorithms comprises three inputs and four outputs (Table 3). The datasets for the output parameters are stored in separate files. In this study, the Waikato environment for knowledge analysis (WEKA) software was used for the ML implementation. WEKA is a Java-language ML tool for implementing algorithms, data analysis, and data mining tasks [46]. Once the dataset was loaded into WEKA, fundamental statistics, such as minimum and maximum values, mean, and standard deviation, were computed. Subsequently, subsets of the data were tested using all applicable regression algorithms available in WEKA. The methodology for ML is illustrated in Figure 2. This diagram summarizes the process of output prediction and accuracy evaluation using an ML-based regression method for 3D-printed materials. Initially, the input data and properties of the 3D-printed material are used as inputs for the model. These data are processed through the ML regression method to produce the predicted output. The results predicted by the model are then compared with actual experimental data to evaluate accuracy. This process enhances the predictive power and performance of the model.

TABLE 2 | Input parameters and level values of the ML algorithm.

Parameter	Symbol	Units	Level 1	Level 2	Level 3
Layer thickness	LT	(μm)	100	150	200
Infill density	ID	%	50	75	100
Nozzle temperature	NT	(°C)	220	230	240

3.2 | Proposed ML Algorithm

In this study, an ML model was proposed to predict various mechanical properties (hardness, tensile strength, surface roughness, and flexural strength) using critical printing parameters (LT, ID, and NT) in the 3D printing process. The methodology adopted for the ML process is illustrated in Figure 3. Initially, the data were normalized between 0 and 1 to enhance classification efficiency. Normalization involves scaling all data values to a specific range, typically to minimize differences in scale among variables and improve algorithm performance. Following normalization, the data selection phase was conducted, during which training and testing datasets were prepared. A 10-fold cross-validation technique was applied at this stage to ensure balanced separation between the training and test datasets, thereby enhancing the reliability and accuracy of the results. In this study, 75% of the data was allocated for training, while the remaining 25% was reserved for testing. Subsequently, ML algorithms were employed with 25 regression algorithms. A performance analysis was conducted to evaluate the effectiveness of the proposed algorithms, ensuring a comprehensive comparison of their predictive capabilities.

3.3 | Performance Evaluation Metrics

Performance analysis is the process used to evaluate the performance of a model and its ability to generalize. This involves various metrics and methods to assess, compare, and optimize the outcomes obtained during the training and testing phases of the models. In this study, the evaluation metrics applied to the regression models include the MSE, RMSE, MAE, and R^2. The MSE was calculated by taking the average of the squared

TABLE 3 | Measured responses: Dataset for the experiments.

	Input parameters			Output parameters			
No	Layer thickness (μm)	Infill density (%)	Nozzle temperature (°C)	Hardness	Flexural strength (MPa)	Tensile strength (MPa)	Roughness (μm)
1	100	50	220	47.63	34.48	25.76	12.87
2	100	50	230	50.68	36.15	26.95	14.08
3	100	50	240	54.08	37.82	28.35	15.46
4	100	75	220	52.13	40.43	31.05	12.18
5	100	75	230	56.10	42.36	32.79	13.38
6	100	75	240	59.81	44.32	34.52	14.65
7	100	100	220	57.39	47.49	38.01	11.59
8	100	100	230	61.23	49.53	40.06	12.65
9	100	100	240	65.21	51.62	42.57	13.85
10	150	50	220	44.29	31.98	23.95	15.46
11	150	50	230	47.06	33.39	24.36	16.89
12	150	50	240	50.03	34.78	25.49	18.43
13	150	75	220	48.86	37.63	28.03	14.68
14	150	75	230	52.15	39.28	29.45	16.12
15	150	75	240	55.47	40.96	30.89	17.65
16	150	100	220	54.26	43.75	34.57	13.97
17	150	100	230	57.68	45.68	36.62	15.32
18	150	100	240	61.43	47.59	38.54	16.83
19	200	50	220	41.95	30.18	21.47	17.79
20	200	50	230	44.58	31.38	22.59	19.52
21	200	50	240	47.49	32.65	23.68	21.35
22	200	75	220	46.37	35.08	26.29	16.89
23	200	75	230	49.35	36.69	27.58	18.59
24	200	75	240	52.57	38.29	28.83	20.35
25	200	100	220	51.29	40.85	32.24	16.12
26	200	100	230	54.68	42.65	33.95	17.68
27	200	100	240	58.09	44.56	35.89	19.45

differences between the predicted and actual values. This calculation emphasizes the magnitude of errors by squaring the differences, which penalizes larger errors more heavily. A lower MSE value indicates that the model's predictions are closer to the actual values, which indicates better performance. However, due to the squared units of the MSE, its interpretation can be challenging; therefore, the square root of the MSE (RMSE) is often used for easier interpretation and comparison.

$$\mathrm{MSE} = \frac{1}{n}\sum_{i=1}^{n}\left(y_i - \hat{y}_i\right)^2 \quad (1)$$

The MAE is calculated by averaging the absolute differences between the predicted and actual values. After summing the absolute differences, the total is divided by the number of data points to obtain the average error. Unlike MSE, MAE does not penalize larger errors more heavily; each error contributes equally, regardless of its magnitude. Therefore, the MAE is particularly suitable in scenarios in which penalizing large errors is not desirable. A lower MAE value indicates that the model's predictions are closer to the actual values.

$$\mathrm{MAE} = \frac{1}{N}\sum_{i=1}^{N}\left|y_i - \hat{y}_i\right| \quad (2)$$

TABLE 4 | Full forms of all algorithms.

Algorithm	Full form
LR	Linear regression model
GP	Gaussian process
MLP	Multi-layer perceptron
SLR	Simple linear regression
SMOREG	Sequential minimal optimization regression
IBK	Instance-based K (K-Nearest neighbors)
KSTAR	K* (instance-based learner)
LWL	Locally weighted learning
AR	Association rules
BAGGİNG	Bootstrap aggregating
CVP	Cross-validation predictor
MS	Model selection
RC	Ridge classifier
RFC	Random forest classifier
RSS	Random subspace
RBD	Reduced error pruning decision tree
IMC	Iterative model construction
DT	Decision tree
M5R	M5' rules
ZeroR	Zero rule
DS	Decision stump
M5P	M5' model tree
RandomF	Random forest
RandomT	Random tree
RepTree	Reduced error pruning tree

The RMSE was computed as the square root of the mean of the squared differences between the predicted and actual values. This metric highlights the magnitude of errors by squaring the differences and subsequently takes the square root to ensure that the error units are consistent with the original data. A lower RMSE value indicates that the model's predictions are closer to the actual values, which reflects better model performance. The RMSE is intuitive and straightforward to interpret, making it a widely used measure for understanding the magnitude of prediction errors.

$$\mathrm{RMSE} = \sqrt{\frac{1}{n}\sum_{i=1}^{n}\left(y_i - \hat{y}_i\right)^2} \tag{3}$$

The R^2 coefficient, also known as the coefficient of determination, is a performance metric that indicates how well a model explains the variability of the dependent variable. R^2 measures how accurately predicted values approximate actual values. It takes a value between 0 and 1, where values closer to 1 indicate that the model explains a larger portion of the variability in the dependent variable. An R^2 value of 1 implies that the model perfectly explains all variability, whereas an R^2 value of 0 indicates that the model fails to explain any variability.

$$R^2 = 1 - \frac{\sum\left(y_i - \hat{y}_i\right)^2}{\sum\left(y_i - \bar{y}\right)^2} \tag{4}$$

4 | Results and Discussion

4.1 | ANOVA Results

In this study, ANOVA was applied to investigate the relationship between input printing parameters, such as LT, ID, and NT, and output parameters, such as hardness, flexural strength, tensile strength, and roughness. ANOVA is a statistical test used to understand the effects of independent variables on dependent variables. This analysis was used to evaluate the influence of each input parameter on the output parameters (Table 5). The *F*-test and *p*-value were examined. The *F*-test measures the contribution of each variable to the variance of the model and determines whether the effects of the input parameters are significant. A high *F* value indicates that the parameter has a significant impact on the dependent variable. The *p*-value, on the other hand, is used to statistically assess this impact. Generally, if the *p*-value is below 0.05, the parameter has a statistically significant effect on the output parameter. As a result of this analysis, the significant effects of input parameters on outcome variables were evaluated, and the relationships between these parameters were elucidated.

When examining the *p*-values, the selected printing parameters were highly significant in terms of their impact on the mechanical properties and surface roughness. However, due to differences in *F*-values, the contribution levels of these parameters substantially vary. The calculated contribution values for each parameter are presented in Table 6. For the Shore D hardness parameter, the most influential factor was ID, which contributed 55.56%. Similar results were observed for the flexural strength and tensile strength parameters, where the ID was again identified as the most impactful factor. In contrast, for the roughness parameter, the most significant factor was the LT, which contributed 70.89%, while the ID had the lowest impact.

Regression coefficients and effect signs derived from the ANOVA results were used to determine whether a factor has a positive (enhancing) or negative (diminishing) effect (Equations (5–8)). The model aims to identify the main and interactional effects of printing parameters on mechanical properties. In regression models, positive coefficients indicate that an increase in the associated model terms enhances the parameter, whereas negative coefficients suggest that an increase in these terms reduces the parameter. The model in Equations (5–7) show that the positive coefficient values for ID and NT imply a gradual increase in hardness, flexural strength, and tensile strength from lower to higher levels. Conversely, because the LT parameter has a negative coefficient, its increase reduces the mechanical properties. In

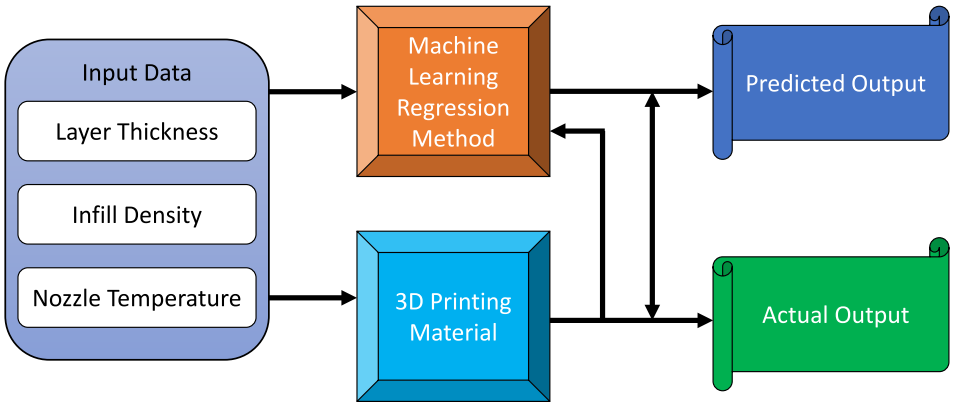

FIGURE 2 | Method of ML for 3D printed material. [Color figure can be viewed at wileyonlinelibrary.com]

Equation (8), it is observed that an increase in the LT parameter results in higher surface roughness.

$$\text{Hardness} = -29.95 - 0.064\,\text{LayerThickness} + 0.207\text{Infill Density} + 0.33\text{NozzleTemperature} \quad (5)$$

$$\text{FlexuralStength} = -9.4 - 0.05\text{LayerThickness} + 0.24\text{InfillDensity} + 0.17\text{NozzleTemperature} \quad (6)$$

$$\text{TensileStength} = -14.8 - 0.05\text{LayerThickness} + 0.24\text{InfillDensity} + 0.15\text{NozzleTemperature} \quad (7)$$

$$\text{Roughness} = -23.2 + 0.052\text{LayerThickness} - 0.031\text{InfillDensity} + 0.147\text{NozzleTemperature} \quad (8)$$

4.2 | Error Performance Metrics Results

In this section, the prediction performances of various ML algorithms on four different output parameters are compared using the MAE, MSE, and RMSE values (Table 7). MAE represents the average of the absolute differences between the predicted and actual values, while MSE squares the errors, penalizing larger errors more heavily. The RMSE is calculated by taking the square root of the MSE, thereby emphasizing the magnitude of the errors.

The algorithm with the lowest error rate was KSTAR for Shore D hardness prediction. This algorithm achieved the best performance, with both an MAE of 0.0066 and an RMSE of 0.0101, indicating highly accurate predictions for hardness. MLP (MAE: 0.1662, RMSE: 0.1991) and SMOREG (MAE: 0.1572, RMSE: 0.2245) also produced successful results with low error rates. However, the cross-validation predictor (CVP), MS, and ZeroR algorithms performed the worst, with both the MAE and RMSE values exceeding 6, indicating poor prediction accuracy.

In the flexural strength prediction, the best performances were obtained by the MLP and RSS algorithms. MLP (MAE: 0.1874, RMSE: 0.2202) and SMOREG (MAE: 0.1977, RMSE: 0.3013) demonstrated successful performance with low error values for flexural strength prediction. Although KSTAR provided excellent results for hardness prediction, it was less successful for flexural strength, with an RMSE value exceeding 1. Again, CVP, MS, and ZeroR demonstrated the worst performance, with RMSE values greater than 6.

The best results were again obtained by MLP (MAE: 0.3325, RMSE: 0.3977) and SLR (MAE: 0.3371, RMSE: 0.4165) algorithms for tensile strength predictions. KSTAR, however, showed higher error rates in this category, with an RMSE of 1.3541, falling behind the other algorithms. CVP, MS, and ZeroR once again had the highest error rates, with CVP reaching an RMSE of 5.9294, indicating poor performance in tensile strength prediction. The most successful roughness prediction algorithm was KSTAR (MAE: 0.013, RMSE: 0.0172), which exhibited very low error rates, indicating outstanding performance in roughness prediction. MLP (MAE: 0.046, RMSE: 0.059) also showed strong performance, with very low error values. In contrast, ZeroR, CVP, and MS demonstrated the worst performance, with RMSE values as high as 2.6115, indicating poor accuracy in roughness predictions. In conclusion, the MLP and KSTAR algorithms consistently achieved successful results across multiple parameters with low MAE, MSE, and RMSE values. In contrast, algorithms like CVP, MS, and ZeroR generally exhibit high error rates and the lowest prediction performance. The best-performing algorithms for each output are indicated in bold in Table 7. These results emphasize the significant impact of selecting an appropriate algorithm on model prediction accuracy.

The MAE and MSE values obtained from ML algorithms have been graphically presented for better representation. The first four graphs illustrate the MAE values (Figure 4a–d). In the hardness and roughness predictions, the MLP and KSTAR algorithms demonstrated low error rates, whereas the CVP, ZeroR, and IMC algorithms exhibited the highest error rates. For the flexural and tensile strengths, MLP and SMOREG demonstrated successful performance with low error rates, whereas CVP and ZeroR demonstrated the worst performance with high error rates. The last four graphs depict the MSE values (Figure 4e–h). MLP and KSTAR algorithms emerged as successful algorithms with very low error rates across all parameters. CVP, MS, and ZeroR exhibit the worst performance, consistently showing high MSE values across all four parameters. The KSTAR algorithm achieved the best hardness predictions with an MAE of 0.0066 and an MSE of 0.0001. Similarly, the roughness results were most accurately predicted using the KSTAR algorithm, with an MAE of 0.013 and an MSE of 0.0003. The best predictions for the flexural and tensile strengths were made by the MLP algorithm.

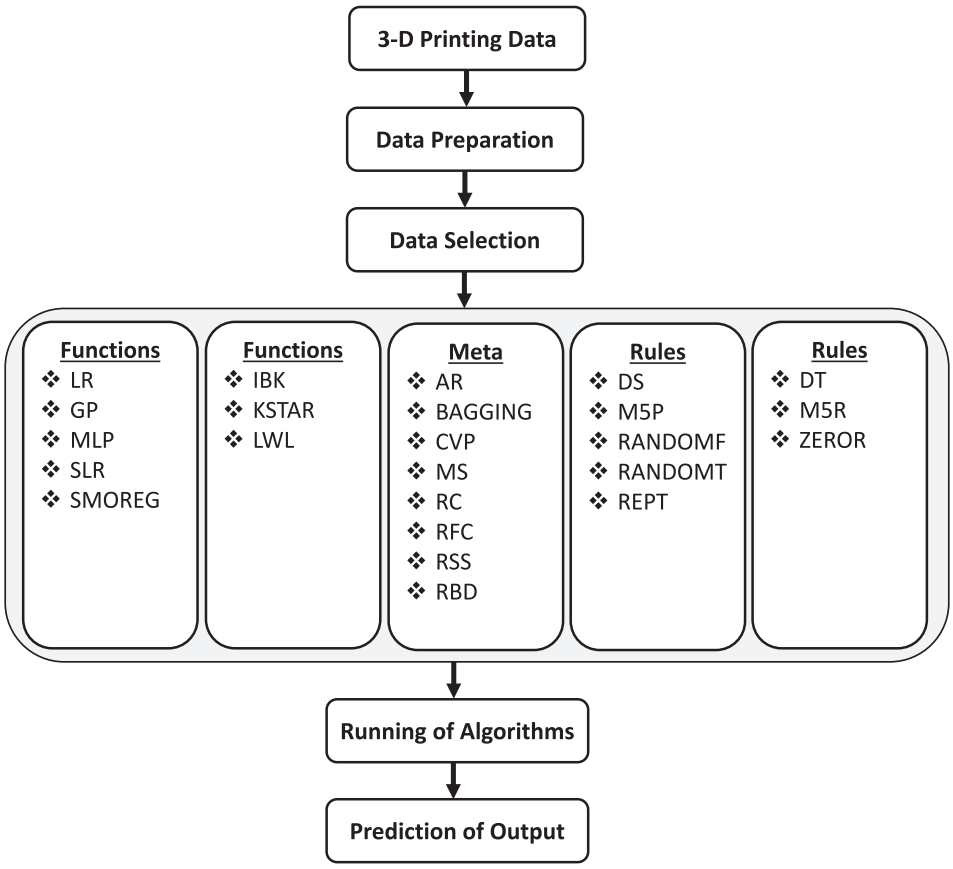

FIGURE 3 | The proposed machine learning flowchart.

TABLE 5 | ANOVA results for input–output parameters.

	Hardness		Flexural strength		Tensile strength		Surface roughness	
Factors	***F***	***p***	***F***	***p***	***F***	***p***	***F***	***p***
Layer thickness	627.83	0.000	328.21	0.000	202.92	0.000	1337.73	0.000
Infill density	1626.68	0.000	1494.56	0.000	1079.05	0.000	125.17	0.000
Nozzle temperature	670.32	0.000	114.53	0.000	66.66	0.000	423.69	0.000
Degree of freedom	26		26		26		26	

TABLE 6 | Contribution values of ANOVA results.

Factors	Hardness	Flexural strength	Tensile strength	Surface r+oughness
Layer thickness	21.48%	16.94%	15.05%	70.89%
Infill density	55.56%	77.13%	80.02%	6.63%
Nozzle temperature	22.92%	5.91%	4.94%	22.47%

The MAE and MSE values for the flexural strength were 0.1874 and 0.048, respectively, while those for the tensile strength were 0.3325 and 0.158. These results indicate that MLP and KSTAR are the most successful algorithms for predicting mechanical properties and surface roughness, achieving the lowest error rates across these metrics, whereas simpler algorithms like ZeroR and CVP demonstrate poor predictive performance.

4.3 | Coefficient of Determination Results

In this section, the performance of various ML algorithms for four criteria (hardness, flexural strength, tensile strength, and roughness) is compared using the coefficient of determination (R^2) values. The results are presented in Table 8. The R^2 values indicate the proportion of variance in the dependent variable

TABLE 7 | MAE, MSE, and RMSE of all algorithms.

Algorithms	Hardness			Flexural strength			Tensile strength			Roughness		
	MAE	MSE	RMSE	MAE	MSE	RMSE	MAE	MSE	RMSE	MAE	MSE	RMSE
LR	0.2346	0.088	0.2982	0.2909	0.125	0.3543	0.3744	0.211	0.4594	0.162	0.0368	0.1919
GP	1.8954	5.179	2.2759	1.7489	4.666	2.1602	1.8395	4.822	2.196	0.813	0.9577	0.9786
MLP	0.1662	0.039	0.1991	**0.1874**	**0.048**	**0.2202**	**0.3325**	**0.158**	**0.3977**	0.046	0.0035	0.059
SLR	1.3512	2.509	1.584	0.3454	0.181	0.4264	0.3371	0.173	0.4165	1.167	1.9063	1.3807
SMOREG	0.1572	0.050	0.2245	0.1977	0.090	0.3013	0.3392	0.202	0.4497	0.141	0.0344	0.1854
IBK	3.2633	10.82	3.2899	1.7033	2.967	1.7225	1.4948	2.463	1.5696	1.452	2.1583	1.4691
KSTAR	**0.0066**	**0.0001**	**0.0101**	0.9315	1.345	1.1621	1.041	1.833	1.3541	**0.013**	**0.0003**	**0.0172**
LWL	3.0243	11.939	3.4553	2.5271	8.999	2.9999	2.4408	8.502	2.9159	1.463	3.0026	1.7328
AR	2.3682	0.6381	0.7988	1.6927	4.927	2.2197	1.8009	4.113	2.0282	0.670	7.221	2.6872
BAGGİNG	2.4192	8.0236	2.8326	1.3807	3.664	1.9144	1.3335	3.455	1.859	1.213	2.2819	1.5106
CVP	5.0443	36.709	6.0588	5.1689	36.99	6.0825	5.0788	35.15	5.9294	2.204	6.8199	2.6115
MS	4.7031	36.709	6.0588	5.1689	36.99	6.0828	5.0788	35.15	5.9294	2.204	6.8199	2.6115
RC	1.9232	5.1475	2.2688	1.2042	2.068	1.4381	1.1517	1.808	1.3448	1.391	2.5751	1.6047
RFC	3.3833	11.688	3.4188	2.4733	8.768	2.9611	2.2015	7.503	2.7392	1.498	2.4264	1.5577
RSS	1.1265	2.0076	1.4169	0.4636	0.515	0.7071	0.6299	0.766	0.8755	1.096	1.7022	1.3047
RBD	0.8412	1.1597	1.0769	0.5518	0.444	0.6668	0.7218	0.730	0.8549	0.661	0.7211	0.8492
IMC	5.0443	36.709	6.0588	5.1689	36.99	6.082	5.0788	35.15	5.9294	2.204	6.8199	2.6115
DT	2.2122	7.0671	2.6584	1.5895	3.962	1.9905	1.477	3.320	1.8222	0.809	0.9716	0.9857
M5R	0.3489	0.1982	0.4452	0.2836	0.134	0.3664	0.3656	0.209	0.4582	0.365	0.2657	0.5155
ZeroR	5.0443	36.709	6.0588	5.1689	36.99	6.082	5.0788	35.15	5.9294	2.204	6.8199	2.6115
DS	3.6173	18.630	4.3163	2.6411	10.295	3.2087	2.7295	10.70	3.2724	1.793	4.4192	2.1022
M5P	0.3489	0.1982	0.4452	0.2836	0.1342	0.3664	0.3539	0.195	0.4423	0.372	0.2674	0.5171
RandomF	1.8989	5.0922	2.2566	0.8232	1.281	1.1318	0.8737	1.455	1.2066	1.168	1.9864	1.4094
RandomT	3.0324	11.337	3.3671	1.9256	5.790	2.4064	1.8778	4.766	2.1833	1.364	2.5132	1.5853
RepTree	3.0506	12.022	3.4674	1.9009	5.349	2.3129	2.3121	7.046	2.6546	1.392	2.7569	1.6604

Note: Bold values represent the algorithms with the lowest error values for each output parameter.

explained by the model. An R^2 value closer to 1 indicates a better-fitting model.

The hardness values indicate that the highest performance was achieved by the KSTAR algorithm (0.9997), followed closely by MLP, SMOREG, and M5P algorithms. These algorithms are highly successful in Shore D hardness prediction. On the other hand, the performance of algorithms such as IBK, ZeroR, and MS was considerably low, as their R^2 values were below 0.5. For flexural strength, the most successful algorithm was the MLP with an almost perfect result (0.9999). Other algorithms like M5R and SMOREG, also exhibit very high performance. However, the performance of algorithms such as IMC and ZeroR, on this metric is quite poor. In terms of tensile strength, MLP again delivers the best result, while the KSTAR, M5P, and RBD algorithms also demonstrate similarly high tensile strength. In contrast, LWL, CVP, and ZeroR yield relatively low results for this metric. Regarding roughness, the KSTAR (0.9999) and MLP (0.9940) algorithms were the best. The LR, SMOREG, and M5P algorithms also performed well on this metric. However, the performance of algorithms like ZeroR, LWL, and IMC is subpar.

MLP, SMOREG, M5P, and KSTAR perform exceptionally well across all four metrics, while ZeroR, IMC, and LWL demonstrate low performance on some metrics. When comparing the results of MAE, MSE, and RMSE with the R^2, the most successful prediction algorithms remain consistent. This consistency indicates the success of the modeling and prediction processes. The results suggest that more complex models generally yield better results in regression problems, although simpler models may still be adequate in certain cases. The regression graphs of the algorithms that successfully predicted the output parameters are presented in Figure 5. Although KSTAR was successful

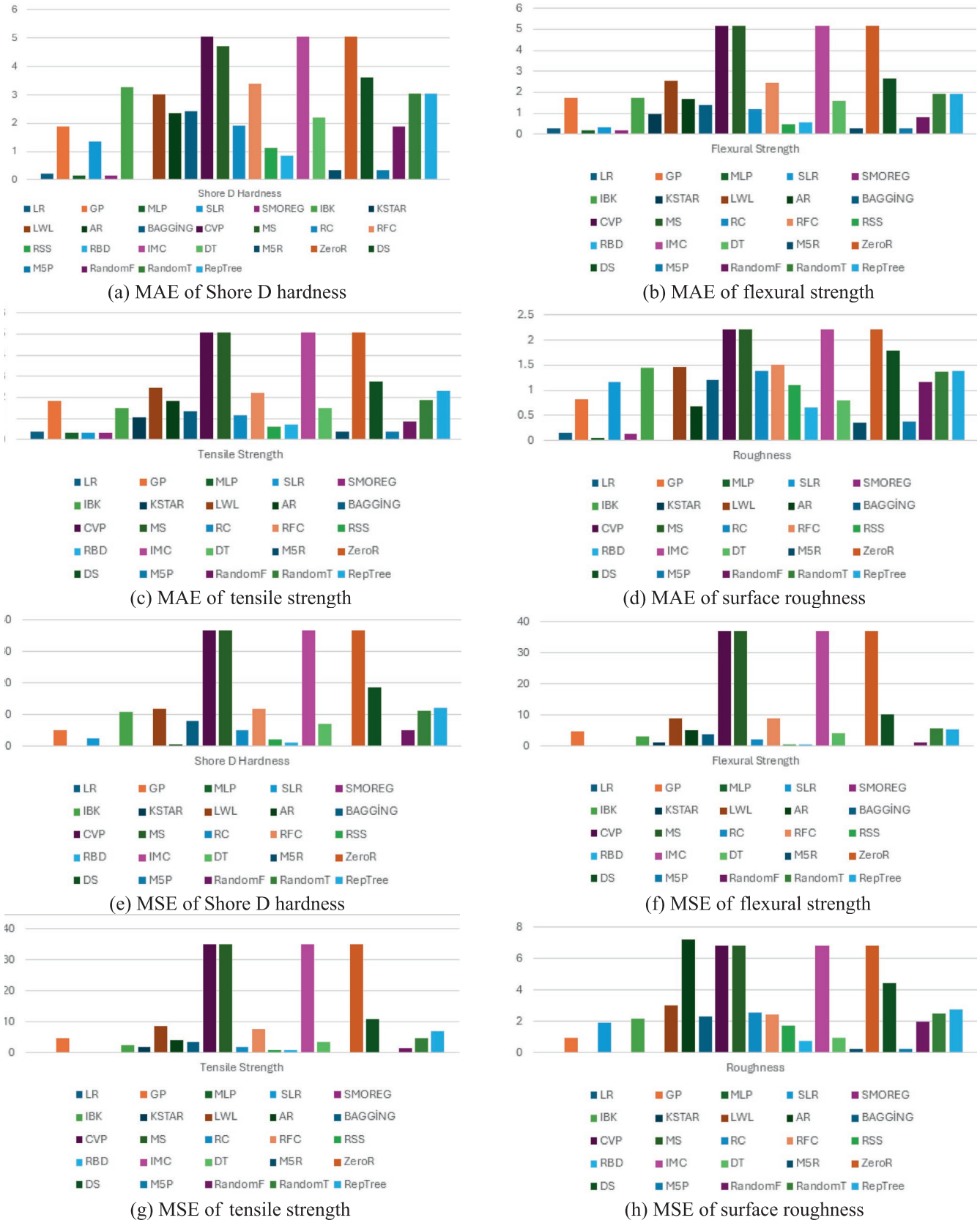

(a) MAE of Shore D hardness

(b) MAE of flexural strength

(c) MAE of tensile strength

(d) MAE of surface roughness

(e) MSE of Shore D hardness

(f) MSE of flexural strength

(g) MSE of tensile strength

(h) MSE of surface roughness

FIGURE 4 | MAE and MSE for predicting mechanical properties and surface roughness. [Color figure can be viewed at wileyonlinelibrary.com]

in predicting hardness and surface roughness, MLP performed best for the flexural and tensile strength parameters. The regression graph is a critical tool for evaluating the accuracy and explaining the variability of prediction models. These graphs help analyze model performance by visualizing how closely predicted values align with actual values.

TABLE 8 | Coefficient of determination of all algorithms.

Algorithms	Shore D strength	Flexural strength	Tensile strength	Roughness
LR	0.992732	0.988632	0.979902	0.993922
GP	0.684201	0.776114	0.801835	0.716248
MLP	0.994895	0.999925	0.999755	0.994047
SLR	0.686539	0.973774	0.985206	0.716248
SMOREG	0.994895	0.993134	0.985206	0.994047
IBK	0.523452	0.776114	0.801835	0.673046
KSTAR	0.999772	0.907817	0.913194	0.999934
LWL	0.570775	0.776114	0.663841	0.562422
AR	0.601762	0.776114	0.801835	0.832858
BAGGİNG	0.601762	0.814997	0.801835	0.701704
CVP	0.570775	0.639338	0.454410	0.682568
MS	0.447010	0.671224	0.474410	0.698759
RC	0.624915	0.814997	0.801835	0.694707
RFC	0.570775	0.776114	0.688891	0.698762
RSS	0.701071	0.971881	0.957070	0.716248
RBD	0.784287	0.916231	0.926983	0.716248
IMC	0.624915	0.612395	0.494410	0.598714
DT	0.624915	0.776114	0.801835	0.716248
M5R	0.944006	0.993134	0.980013	0.851006
ZeroR	0.523452	0.473206	0.454410	0.468742
DS	0.570775	0.681084	0.653685	0.598761
M5P	0.932961	0.991436	0.984806	0.896323
RandomF	0.648300	0.907817	0.913194	0.716248
RandomT	0.570775	0.776114	0.688891	0.694707
RepTree	0.570775	0.776114	0.678980	0.687303

In each graph, the red line represents the ideal scenario (where predicted values perfectly match the actual values), and the blue dots represent the relationship between actual and predicted values. The R^2 values displayed in the graphs indicate how well the models perform, with an R^2 value close to 1 indicating a highly successful model. Figure 5a shows hardness predictions made using the KSTAR algorithm. The R^2 value is 0.9997726, indicating an almost perfect fit. The blue dots are distributed very closely around the red line, indicating that the predicted values are nearly equal to the actual values. This suggests that the KSTAR algorithm accurately predicted the Shore D hardness parameter. The MLP algorithm is used to predict the flexural strength (Figure 5b). The R^2 value is 0.999925, demonstrating that the algorithm achieved almost flawless performance. The blue dots are aligned very closely and parallel to the red line. This confirms that the MLP algorithm is highly effective in predicting flexural strength. Figure 5c shows the performance of the MLP algorithm in predicting the tensile strength. The R^2 value is 0.999755, again indicating an almost perfect fit. The blue dots are distributed very close to the red line in a well-aligned pattern. This demonstrates the MLP algorithm's excellent predictive ability for this metric. Finally, surface roughness predictions are presented in Figure 5d using the KSTAR algorithm, with an R^2 value of 0.999934. This high value highlights the model's exceptional performance. The blue dots are once again very close to the red line, demonstrating that the model predictions are almost identical to the actual roughness values. Thus, the KSTAR algorithm is also highly effective in predicting roughness. The regression graphs in Figure 5 demonstrate the impressive predictive power of both the KSTAR and MLP algorithms across different metrics. The near-perfect R^2 values in all cases indicate that these models achieved a high degree of accuracy in predicting.

4.4 | Predicted Versus Actual Results

The predicted vs. actual graph is a tool used to visualize the relationship between the values predicted by a model or analysis

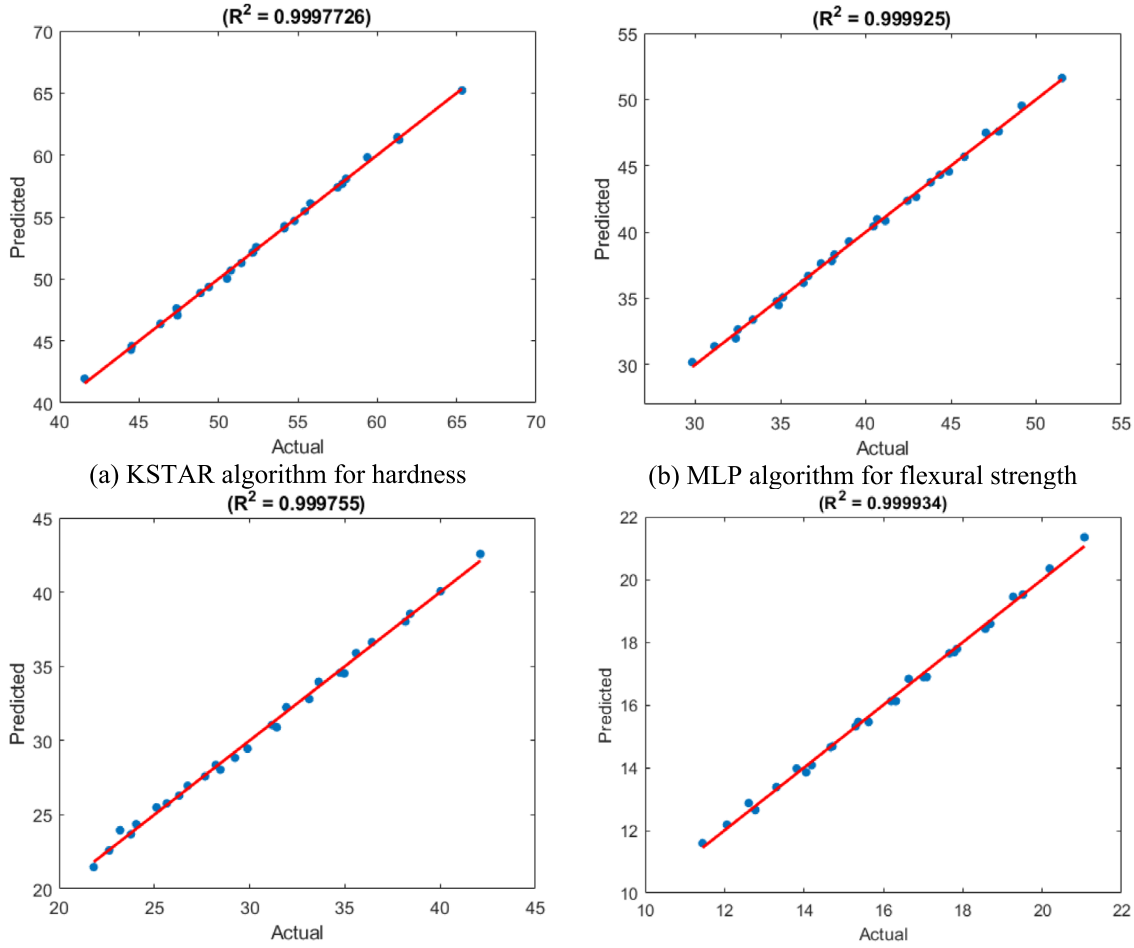

FIGURE 5 | Regression graphs of the most successful machine learning algorithms. [Color figure can be viewed at wileyonlinelibrary.com]

method and the actual observed values. In each graph, red and blue points represent the predicted and actual values, respectively. This type of graph is commonly used to evaluate model accuracy and performance. In this section, the graphs were created using 27 data points derived from the outputs of the best prediction methods. Figure 6 compares the predicted and actual values for Shore D hardness, flexural strength, tensile strength, and surface roughness. Figure 6a shows that the predicted Shore D hardness values are generally very close to the actual values, with minor deviations in some cases. However, the overall trend indicates that the model performs well at predicting hardness. Similarly, in Figure 6b, the flexural strength predictions align closely with the actual values, showing minimal discrepancies between the two. In Figure 6c, the tensile strength predictions demonstrate a high degree of proximity to the actual values, although minor deviations are observed in a few cases. For surface roughness, as depicted in Figure 6d, the predicted values exhibit strong agreement with the actual values, even in instances of small differences, maintaining the overall trend. These findings highlight the model's high predictive performance and its ability to provide accurate estimates for various mechanical properties. Across all graphs, a general concordance between the predicted and actual values is evident. The red and blue points mostly overlap or are positioned in proximity. This indicates that the ML models performed with high accuracy in predicting both the mechanical properties and surface roughness. Although minor deviations were observed in some experiments, the models can be considered successful in their overall predictions.

The varying performance of ML models in this study can be attributed to several factors related to the characteristics of the algorithms and the nature of the dataset. First, certain algorithms, such as ZeroR and CVP, demonstrated poor performance because they lacked the complexity required to capture the intricate relationships between the input parameters (LT, ID, and NT) and the output mechanical properties. ZeroR only predicts the value of the dependent variable without considering the input features, making it unsuitable for datasets with non-linear relationships. Similarly, simpler models like LWL and IMC struggled because of their limited ability to generalize from the provided data, especially in cases where interactions between parameters were significant. Conversely, more complex algorithms like MLP and KSTAR performed exceptionally well due to their ability to model non-linear relationships and capture subtle patterns in the data. Algorithms like MLP, which use neural networks, excel in handling multidimensional datasets and can adapt to the inherent variability in mechanical properties. Algorithms such as IBK and RandomT, which rely on instance-based or random tree approaches, may have underperformed due to their sensitivity to the small size of the dataset. These models tend to overfit when

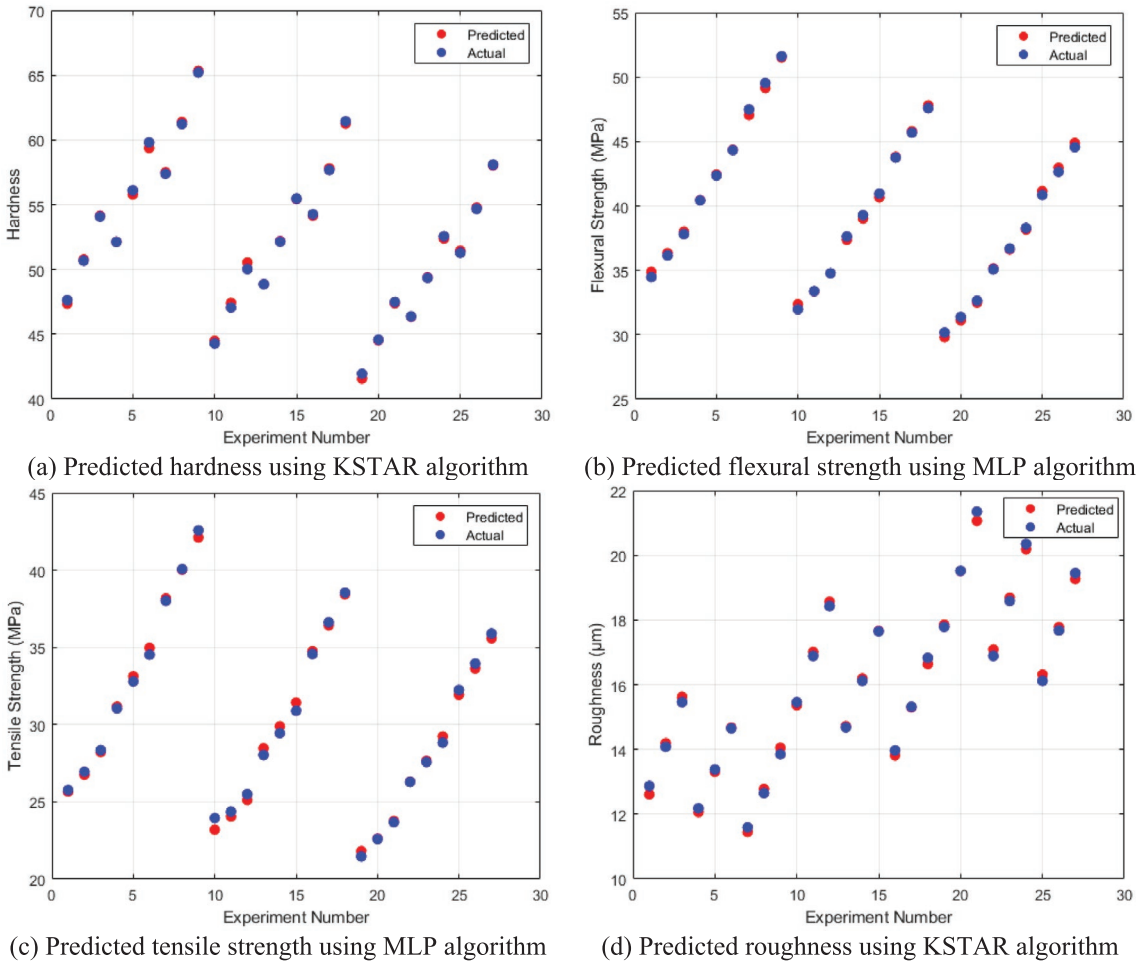

(a) Predicted hardness using KSTAR algorithm

(b) Predicted flexural strength using MLP algorithm

(c) Predicted tensile strength using MLP algorithm

(d) Predicted roughness using KSTAR algorithm

FIGURE 6 | Predicted mechanical properties and surface roughness versus actual values. [Color figure can be viewed at wileyonlinelibrary.com]

the dataset is limited, leading to reduced prediction accuracy on unseen data. In addition, the quality of results is influenced by the specific design and assumptions of each algorithm. Tree-based models like RF and RepTree are effective in handling non-linear data but may face limitations in extrapolating beyond the range of the training data. Similarly, methods like SMOREG, while generally effective, may struggle with datasets where the variance in certain output variables is relatively small, as seen in surface roughness predictions.

An important observation from this study is that different algorithms excel in predicting different mechanical properties. As an illustration, KSTAR excelled in hardness and surface roughness predictions, whereas MLP proved to be more effective in forecasting tensile and flexural strength. This variation underscores the fact that no single algorithm is universally optimal for all types of data or target variables. The differences can be attributed to the nature of the parameters being analyzed and the inherent strengths of the algorithms. For example, KSTAR, being an instance-based algorithm, is well suited for capturing localized patterns in the data, making it effective for surface roughness and hardness, which are highly sensitive to specific parameter interactions. In contrast, MLP's neural network architecture enables it to model complex, non-linear relationships across the entire dataset, which explains its superior performance for tensile and flexural strength. This study highlights the need for a systematic approach to selecting algorithms that are best suited for specific datasets and prediction tasks. Although the results offer valuable insights into the performance of different ML models, practical application in real-world scenarios requires a method for determining the most appropriate algorithm in advance. Future study could focus on developing a meta-learning approach that examines dataset characteristics, such as feature distributions, dimensionality, and the degree of nonlinearity, to predict the most suitable algorithm for a given task. For instance, analyzing the variance, correlation structure, or complexity of the input–output relationships could provide a basis for automated model selection. Such a framework would significantly enhance the utility of ML in real-world applications, enabling users to select the best algorithm without the need for extensive trial-and-error experimentation. Furthermore, understanding why certain algorithms perform better for specific parameters requires a deeper investigation into the interaction between parameter characteristics and algorithm architecture. Surface roughness and hardness may be better predicted by algorithms that focus on localized relationships, while tensile and flexural strength might benefit from models capable of capturing global patterns across the dataset. Exploring such relationships in future studies could provide

valuable guidelines for both selecting and designing ML models tailored to specific FDM applications.

In summary, the differences in algorithm performance can be justified by the balance between model complexity, dataset size, and the ability to capture non-linear or interaction effects. Although some models are inherently better suited for capturing complex relationships, others are limited by their simplicity or sensitivity to dataset characteristics. These findings highlight the importance of selecting appropriate ML models based on both the nature of the data and the desired prediction accuracy. In addition, the development of a systematic framework for algorithm selection based on dataset characteristics and parameter-specific requirements would be a valuable direction for future research, further enhancing the practical applicability of ML in FDM processes.

4.5 | Discussion

The findings of this study demonstrate the successful application of ML algorithms in predicting the mechanical properties of FDM-produced ABS parts. The high accuracy achieved by the KSTAR algorithm in predicting Shore D hardness ($R^2 = 0.9997$) and surface roughness ($R^2 = 0.9993$), along with the MLP algorithm's superior performance in predicting tensile strength ($R^2 = 0.9997$) and flexural strength ($R^2 = 0.9999$), validates the robustness of these approaches within the experimental domain established. Regarding the generalizability of these models, several important considerations emerge. While the models show exceptional performance within the specified parameter ranges (LT: 100–200 μm, ID: 50%–100%, NT: 220°C–240°C), their applicability to broader FDM operations requires careful examination. The models' predictive capabilities are inherently influenced by the specific material properties of ABS and the defined experimental conditions. However, the underlying principles and methodologies can be adapted to similar FDM applications with appropriate modifications.

The transferability of these models to other FDM operations depends on several factors. First, the physical and chemical properties of the printing material significantly influence the mechanical properties. While these models might be directly applicable to ABS-based applications within similar parameter ranges, extending them to other materials (such as PLA, PETG, or composite materials) would require retraining with material-specific data. Second, the printing parameters used in this study, while comprehensive, represent a subset of the possible FDM process parameters. Additional factors such as PS, bed temperature, raster angle, and environmental conditions could affect the mechanical properties in ways not captured by the current models. The ANOVA results provide valuable insights into the relative importance of different parameters, with ID showing the highest impact on mechanical properties (55.56%–80.02%) except for surface roughness. This understanding of parameter significance could be generalized to guide parameter selection in other FDM applications, even when using different materials or equipment. However, specific quantitative relationships might vary depending on the material and process conditions. The ML approaches demonstrated in this study offer a framework that could be adapted for other FDM applications. The success of the KSTAR and MLP algorithms suggests that these methods can effectively capture the complex relationships between printing parameters and mechanical properties. The methodology of using multiple algorithms and selecting the best-performing ones based on comprehensive error metrics (MAE, RMSE, MSE, R^2) provides a robust approach that could be replicated for different FDM applications.

In addition to these findings, it is essential to discuss the practical applications of ML in FDM processes, as highlighted by this study. The developed ML models can be utilized in real-world manufacturing as optimization tools for determining printing parameter combinations that achieve specific mechanical property requirements. For instance, in a production line, where a particular application demands minimum surface roughness or maximum tensile strength, these models could quickly identify the optimal parameter settings. This application would significantly reduce the time and costs associated with trial-and-error experiments. One critical aspect not directly addressed in this study is the comparison between the use of ML techniques and the expertise of experienced operators. While experienced operators can often determine effective global parameter settings based on their knowledge and intuition, ML provides an opportunity to systematically optimize these parameters, particularly in situations where new materials are being introduced or where the relationships between parameters and outcomes are highly complex. ML models, as demonstrated in this study, can provide a quantitative and repeatable framework for optimization, reducing the dependency on individual expertise and minimizing the risk of human error. When working with novel materials with minimal existing data, refining ML models with targeted material-specific information can ensure efficient and precise parameter optimization. The choice of the algorithm in such scenarios would depend on the complexity of the material behavior and the desired mechanical outcomes, as discussed earlier. Moreover, this study primarily focuses on global parameter optimization, where the same parameter values are applied throughout the print. However, as highlighted in previous studies [47], local optimization—where parameters are varied dynamically during the printing process—can often result in superior outcomes, particularly for complex geometries or multifunctional parts. Although local optimization was beyond the scope of this study, it represents a promising avenue for future research. The integration of ML models into real-time control systems could enable dynamic adjustments to parameters such as NT or ID in response to changing conditions during the print. Such an approach would leverage the predictive power of ML to achieve not only global but also localized optimization, further enhancing the precision and efficiency of FDM processes. Another potential application lies in customized manufacturing processes. For example, in the medical field, where personalized prosthetics or implants are produced, ML models could optimize printing parameters to meet specific mechanical and surface quality requirements, improving the efficiency and precision of such processes. Despite these promising applications, certain challenges must be addressed to ensure the successful industrial integration of these models. First, the models must be retrained with broader datasets to accommodate wider parameter ranges and different materials. Second, the development of hybrid models that combine physics-based understanding with ML could enhance predictive accuracy, especially across

varying operating conditions. Finally, user-friendly interfaces and compatibility with real-time data systems would be crucial for seamless industrial implementation.

In conclusion, while the models developed in this study show excellent predictive capability within the specified experimental domain, their generalization to other FDM operations requires careful consideration of material properties, process parameters, and operating conditions. The methodology and insights gained from this study provide a valuable foundation for developing similar predictive models for other FDM applications, but the direct application of the current models should be approached with appropriate validation and potential adaptation to specific use cases. In addition, exploring the integration of ML for local parameter optimization and dynamic control during the printing process represents an important direction for future work. The high accuracy achieved suggests that ML approaches can effectively predict mechanical properties in FDM processes, potentially reducing the need for extensive experimental testing and paving the way for practical industrial applications.

5 | Conclusions

In this study, 25 different ML algorithms were used to predict the mechanical properties of ABS parts produced using the FDM method, and the effects of printing parameters (LT, ID, and NT) on the mechanical properties were analyzed. According to the ANOVA results, the ID had the greatest impact on hardness (55.56%), tensile strength (80.02%), and flexural strength (77.13%). In contrast, the LT was identified as the most influential parameter on the surface roughness, with a 70.89% effect. The performance of the ML algorithms was evaluated using various error metrics, including MAE, RMSE, MSE, and R^2. For predicting hardness and surface roughness, the KSTAR algorithm achieved the best results, with MAE: 0.006 and R^2: 0.99 for hardness, and MAE: 0.009 and R^2: 0.99 for surface roughness. For the prediction of tensile and flexural strength, the MLP algorithm showed the highest accuracy, with $R^2 > 0.99$ for both properties. The regression graphs demonstrate the performance of the algorithms by comparing the predicted values with the experimental results. The regression graphs for hardness and surface roughness demonstrated that the KSTAR algorithm's predictions were highly consistent with the experimental values, showing a strong correlation. The KSTAR algorithm exhibited remarkable precision in hardness prediction, as the predicted values were nearly identical to the actual data. A similar level of success was observed for the surface roughness prediction, where the predicted and actual values were very close. The regression graphs for tensile and flexural strength prediction highlight the superior performance of the MLP algorithm. The predicted values for both the tensile and flexural strengths closely aligned with the experimental results, showing a strong linear relationship. The $R^2 > 0.99$ values indicated that the model could explain almost all the variation in the data, with the predicted results closely matching the experimental outcomes. In the regression graphs, the predicted and actual values were mostly aligned along a 45° line ($y = x$), further confirming the high accuracy of the model. This study demonstrated the effectiveness of ML algorithms in predicting the mechanical properties of ABS parts produced by FDM and provided recommendations for optimizing printing parameters. The proper selection of parameters such as ID, LT, and NT plays a crucial role in improving the mechanical properties of printed parts. Future studies could explore similar analyses using different materials and production methods, as well as test the performance of ML algorithms on larger datasets.

Author Contributions

Mahmut Özkül: formal analysis (equal), investigation (equal), methodology (equal), resources (equal), software (equal), validation (equal), writing – original draft (equal). **Fatma Kuncan:** conceptualization (equal), formal analysis (equal), investigation (equal), methodology (equal), resources (equal), software (equal), supervision (equal), visualization (equal), writing – original draft (equal). **Osman Ulkir:** conceptualization (equal), formal analysis (equal), investigation (equal), methodology (equal), software (equal), validation (equal), writing – original draft (equal).

Ethics Statement

The authors have nothing to report.

Conflicts of Interest

The authors declare no conflicts of interest.

Data Availability Statement

The data that support the findings of this study are available from the corresponding author upon reasonable request.

References

1. I. Fidan, O. Huseynov, M. A. Ali, et al., "Recent Inventions in Additive Manufacturing: Holistic Review," *Inventions* 8 (2023): 103.

2. P. Badoniya, M. Srivastava, P. K. Jain, and S. Rathee, "A State-Of-The-Art Review on Metal Additive Manufacturing: Milestones, Trends, Challenges and Perspectives," *Journal of the Brazilian Society of Mechanical Sciences and Engineering* 46 (2024): 339.

3. S. Rouf, A. Malik, N. Singh, et al., "Additive Manufacturing Technologies: Industrial and Medical Applications," *Sustainable Operations and Computers* 3 (2022): 258–274.

4. G. Prashar, H. Vasudev, and D. Bhuddhi, "Additive Manufacturing: Expanding 3D Printing Horizon in Industry 4.0," *International Journal on Interactive Design and Manufacturing* 17 (2023): 2221–2235.

5. L. Zhou, J. Miller, J. Vezza, et al., "Additive Manufacturing: A Comprehensive Review," *Sensors* 24 (2024): 2668.

6. T. Vaneker, A. Bernard, G. Moroni, I. Gibson, and Y. Zhang, "Design for Additive Manufacturing: Framework and Methodology," *CIRP Annals* 69 (2020): 578–599.

7. S. Gunes, O. Ulkir, and M. Kuncan, "Application of Artificial Neural Network to Evaluation of Dimensional Accuracy of 3D-Printed Polylactic Acid Parts," *Journal of Polymer Science* 62 (2024): 1864–1889.

8. A. Patel and M. Taufik, "Extrusion-Based Technology in Additive Manufacturing: A Comprehensive Review," *Arabian Journal for Science and Engineering* 49 (2024): 1309–1342.

9. Y. Wang, R. T. Mushtaq, A. Ahmed, et al., "Additive Manufacturing Is Sustainable Technology: Citespace Based Bibliometric Investigations of Fused Deposition Modeling Approach," *Rapid Prototyping Journal* 28 (2022): 654–675.

10. H. Ardeshir, M. Hoseinzadeh, M. B. Limooei, and S. Hosseini, "A Scientometrics Study and Its Practical Implications for Fused Deposition Modeling," *Alexandria Engineering Journal* 99 (2024): 217–231.

11. T. Sathies, P. Senthil, and M. S. Anoop, "A Review on Advancements in Applications of Fused Deposition Modelling Process," *Rapid Prototyping Journal* 26 (2020): 669–687.

12. M. Moradi, A. Aminzadeh, D. Rahmatabadi, and A. Hakimi, "Experimental Investigation on Mechanical Characterization of 3D Printed PLA Produced by Fused Deposition Modeling (FDM)," *Materials Research Express* 8 (2021): 035304.

13. A. Rasheed, M. Hussain, S. Ullah, et al., "Experimental Investigation and Taguchi Optimization of FDM Process Parameters for the Enhancement of Tensile Properties of bi-Layered Printed PLA-ABS," *Materials Research Express* 10 (2023): 095307.

14. M. Algarni and S. Ghazali, "Comparative Study of the Sensitivity of PLA, ABS, PEEK, and PETG's Mechanical Properties to FDM Printing Process Parameters," *Crystals* 11 (2021): 995.

15. I. Khan, I. Barsoum, M. Abas, A. Al Rashid, M. Koç, and M. Tariq, "A Review of Extrusion-Based Additive Manufacturing of Multi-Materials-Based Polymeric Laminated Structures," *Composite Structures* 349–350 (2024): 118490.

16. R. B. Kristiawan, F. Imaduddin, D. Ariawan, Ubaidillah, and Z. Arifin, "A Review on the Fused Deposition Modeling (FDM) 3D Printing: Filament Processing, Materials, and Printing Parameters," *Open Engineering* 11 (2021): 639–649.

17. S. Wickramasinghe, T. Do, and P. Tran, "FDM-Based 3D Printing of Polymer and Associated Composite: A Review on Mechanical Properties, Defects and Treatments," *Polymers (Basel)* 12 (2020): 1529.

18. N. A. Fountas, K. Kitsakis, K.-E. Aslani, J. D. Kechagias, and N. M. Vaxevanidis, "An Experimental Investigation of Surface Roughness in 3D-Printed Pla Items Using Design of Experiments," *Proceedings of the Institution of Mechanical Engineers, Part J: Journal of Engineering Tribology* 236 (2022): 1979–1984.

19. K. Tüfekci, B. G. Çakan, and V. M. Küçükakarsu, "Stress Relaxation of3DprintedPLAof Various Infill Orientations Under Tensile and Bending Loadings," *Journal of Applied Polymer Science* 140 (2023): 140.

20. N. Ben Ali, M. Khlif, D. Hammami, and C. Bradai, "Experimental Optimization of Process Parameters on Mechanical Properties and the Layers Adhesion of3Dprinted Parts," *Journal of Applied Polymer Science* 139 (2022): 139.

21. N. A. Fountas, J. D. Kechagias, D. E. Manolakos, and N. M. Vaxevanidis, "Single and Multi-Objective Optimization of FDM-Based Additive Manufacturing Using Metaheuristic Algorithms," *Procedia Manufacturing* 51 (2020): 740–747.

22. J. D. Kechagias, S. P. Zaoutsos, N. A. Fountas, and N. M. Vaxevanidis, "Experimental Investigation and Neural Network Development for Modeling Tensile Properties of Polymethyl Methacrylate (PMMA) Filament Material," *International Journal of Advanced Manufacturing Technology* 134 (2024): 4387–4398.

23. J. Kechagias and S. Zaoutsos, "Effects of 3D-Printing Processing Parameters on FFF Parts' Porosity: Outlook and Trends," *Materials and Manufacturing Processes* 39 (2024): 804–814.

24. S. Kumar, T. Gopi, N. Harikeerthana, et al., "Machine Learning Techniques in Additive Manufacturing: A State of the Art Review on Design, Processes and Production Control," *Journal of Intelligent Manufacturing* 34 (2023): 21–55.

25. C. Wang, X. P. Tan, S. B. Tor, and C. S. Lim, "Machine Learning in Additive Manufacturing: State-Of-The-Art and Perspectives," *Additive Manufacturing* 36 (2020): 101538.

26. G. D. Goh, S. L. Sing, and W. Y. Yeong, "A Review on Machine Learning in 3D Printing: Applications, Potential, and Challenges," *Artificial Intelligence Review* 54 (2021): 63–94.

27. M. Khalil, A. S. McGough, Z. Pourmirza, M. Pazhoohesh, and S. Walker, "Machine Learning, Deep Learning and Statistical Analysis for Forecasting Building Energy Consumption — A Systematic Review," *Engineering Applications of Artificial Intelligence* 115 (2022): 105287.

28. R. Rai, M. K. Tiwari, D. Ivanov, and A. Dolgui, "Machine Learning in Manufacturing and Industry 4.0 Applications," *International Journal of Production Research* 59 (2021): 4773–4778.

29. A. S. Khusheef, M. Shahbazi, and R. Hashemi, "Deep Learning-Based Multi-Sensor Fusion for Process Monitoring: Application to Fused Deposition Modeling," *Arabian Journal for Science and Engineering* 49 (2024): 10501–10522.

30. T. Sai, V. K. Pathak, and A. K. Srivastava, "Modeling and Optimization of Fused Deposition Modeling (FDM) Process Through Printing PLA Implants Using Adaptive Neuro-Fuzzy Inference System (ANFIS) Model and Whale Optimization Algorithm," *Journal of the Brazilian Society of Mechanical Sciences and Engineering* 42 (2020): 617.

31. O. A. Mohamed, S. H. Masood, and J. L. Bhowmik, "Experimental Study of the Wear Performance of Fused Deposition Modeling Printed Polycarbonate-Acrylonitrile Butadiene Styrene Parts Using Definitive Screening Design and Machine Learning-Genetic Algorithm," *Journal of Materials Engineering and Performance* 31 (2022): 2967–2977.

32. O. Ulkir, M. S. Bayraklılar, and M. Kuncan, "Raster Angle Prediction of Additive Manufacturing Process Using Machine Learning Algorithm," *Applied Sciences* 14 (2024): 2046.

33. A. Cerro, P. E. Romero, O. Yiğit, and A. Bustillo, "Use of Machine Learning Algorithms for Surface Roughness Prediction of Printed Parts in Polyvinyl Butyral via Fused Deposition Modeling," *International Journal of Advanced Manufacturing Technology* 115 (2021): 2465–2475.

34. N. Hooda, J. S. Chohan, R. Gupta, and R. Kumar, "Deposition Angle Prediction of Fused Deposition Modeling Process Using Ensemble Machine Learning," *ISA Transactions* 116 (2021): 121–128.

35. C. Hu, W. N. J. Hau, W. Chen, and Q.-H. Qin, "The Fabrication of Long Carbon Fiber Reinforced Polylactic Acid Composites via Fused Deposition Modelling: Experimental Analysis and Machine Learning," *Journal of Composite Materials* 55 (2021): 1459–1472.

36. P. Charalampous, I. Kostavelis, T. Kontodina, and D. Tzovaras, "Learning-Based Error Modeling in FDM 3D Printing Process," *Rapid Prototyping Journal* 27 (2021): 507–517.

37. O. Ulkir, "3D Print," *Additive Manufacturing* 10 (2023): 1423.

38. Y. Ni, Q. Gao, Z. Hao, et al., "Enhancing the Strength and Toughness of Polylactic Acid Through Fused Deposition Modeling-Induced Orientation and Nucleation Effects of Attapulgite," *Journal of Applied Polymer Science* 141 (2024): 141.

39. B. K. Behera, "Mechanical, Viscoelastic, and Biodegradability Characteristics of Ramie Fibre-Reinforced Acrylonitrile Butadiene Styrene Composites," *Journal of Applied Polymer Science* 141 (2024): 141.

40. Z. G. Mohammadsalih, A. F. Abdulameer, N. S. Sadeq, L. K. Abbas, and S. M. Sapuan, "Preparation, Characterization, and Properties of Acrylonitrile Butadiene Styrene / Multi Walled Carbon Nanotubes Nanocomposites," *Journal of Polymer Research* 31 (2024): 203.

41. J. Zhu, Z. Su, Q. Wang, et al., "Surface Quality Prediction and Quantitative Evaluation of Process Parameter Effects for 3D Printing With Transfer Learning-Enhanced Gradient-Boosting Decision Trees," *Expert Systems with Applications* 237 (2024): 121478.

42. B. El Essawi, S. Abdallah, S. Ali, A. Nassir Abdo Mohammed, R. A. Susantyoko, and S. Pervaiz, "Optimization of Infill Density, Fiber Angle, Carbon Fiber Layer Position in 3D Printed Continuous Carbon-Fiber Reinforced Nylon Composite," *Results in Engineering* 21 (2024): 101926.

43. N. H. Musa, N. N. Mazlan, S. Mohd Yusuf, F. L. Binti Mohd Redzuan, N. A. Nordin, and S. A. Mazlan, "Influence of Nozzle Temperatures on the Microstructures and Physical Properties of 316l Stainless Steel Parts Additively Manufactured by Material Extrusion," *Rapid Prototyping Journal* 30 (2024): 2021–2032.

44. M. El Rajab, L. Yang, and A. Shami, "Zero-Touch Networks: Towards Next-Generation Network Automation," *Computer Networks* 243 (2024): 110294.

45. A. H. Salem, S. M. Azzam, O. E. Emam, and A. A. J. Abohany, "Advancing Cybersecurity: A Comprehensive Review of AI-Driven Detection Techniques," *Big Data* 11 (2024): 105.

46. A. Gupta and N. K. Chauhan, "A Severity-Based Classification Assessment of Code Smells in Kotlin and Java Application," *Arabian Journal for Science and Engineering* 47 (2022): 1831–1848.

47. J. M. Gardner, K. A. Hunt, A. B. Ebel, et al., "Machines as Craftsmen: Localized Parameter Setting Optimization for Fused Filament Fabrication 3D Printing," *Advanced Materials Technologies* 4 (2019): 1800653.